Investigation of basic imaging properties in digital radiography. 12. Effect of matrix configuration on spatial resolution

Hiroshi Fujita,[a] Maryellen Lissak Giger, and Kunio Doi
Kurt Rossmann Laboratories for Radiologic Image Research, Department of Radiology, The University of Chicago, Chicago, Illinois 60637

(Received 30 December 1986; accepted for publication 6 July 1987)

We investigated the effects of three matrix configurations (a conventional 512×512 matrix, a double-sampling matrix, and a high-resolution 1024×1024 matrix) on the resolution properties of an image intensifier (II)–TV digital radiographic imaging system. Expressions for the optical transfer function were derived theoretically for each of the three matrix configurations, and the corresponding digital modulation transfer functions (MTF's) were calculated using the measured MTF's of the presampling analog components and the parameters of the digital system. In addition, digital images of a star pattern phantom and a hand phantom were obtained with the II–TV system for each matrix type. From our results, we conclude that, in order to increase the resolution of an II–TV digital imaging system, it is necessary not only to increase the matrix size, but also to improve the resolution capabilities of analog components such as the II and/or TV camera. In addition, if the system cannot be upgraded to a 1024×1024 matrix configuration, a double-sampling technique with an 512×512 matrix may be employed.

Key words: spatial resolution, matrix size, digital radiography, modulation transfer function, II–TV system

I. INTRODUCTION

The physical quality of a radiographic image depends largely on the resolution properties of the particular imaging system employed. It has been shown, for digital radiographic imaging systems, that the resolution properties depend on various physical parameters (such as the detector, sampling distance, sampling aperture, and display aperture).[1-3] Some of these parameters are related to the matrix configuration used by the system during image acquisition. Gomes *et al.*[4] compared phantom images obtained with a commercial digital subtraction angiography (DSA) unit configured for both 512×512 and 1024×1024 acquisition matrices. They found only modest improvement in the resolution obtained with a 1024×1024 matrix as compared to that obtained with a 512×512 matrix, and they suggested that this small improvement was attributable to factors such as system noise. However, Kamiya *et al.*[5] reported a significant increase in the resolution properties with their DSA system when they employed an improved TV camera and a 1024×1024 matrix. Their results show an almost twofold increase in the resolution limit (in terms of line pairs/mm) over the 512×512 system, as determined with lead bar test patterns.

In this study, we examined the effect of the matrix configuration on the spatial resolution of an image intensifier (II)–TV digital radiographic imaging system. We considered three types of matrix configurations: a conventional 512×512 matrix, a double-sampling matrix, and a high-resolution 1024×1024 matrix. The double-sampling method corresponds to a "double reading" of the II image with a TV camera such that the second reading (or scan) is made at positions shifted by one-half the pixel size from the first scan.[6] In the past, the modulation transfer function (MTF) has been used frequently for quantification and evaluation of the resolution properties of analog[7,8] and digital[1-3,6,9,10] radiographic imaging systems. Thus, we evaluated the resolution properties obtainable with the three matrix configurations by using transfer function analysis to calculate the digital MTF's. In addition, we compared the three matrix configurations qualititatively by using radiographic phantoms.

II. DIGITAL OPTICAL TRANSFER FUNCTIONS

A schematic diagram illustrating the sampling method used with each of the three matrix configurations is shown in Fig. 1. The points indicate the positions at which the continuous image data are sampled. With the double-sampling matrix, the image is scanned twice, as the name implies, first at positions along the solid lines and then at those along the dashed lines. The finest sampling occurs with the 1024×1024 matrix configuration. It should be noted that, as compared to the 512×512 matrix, twice as many sampled points are obtained with the double-sampling matrix and

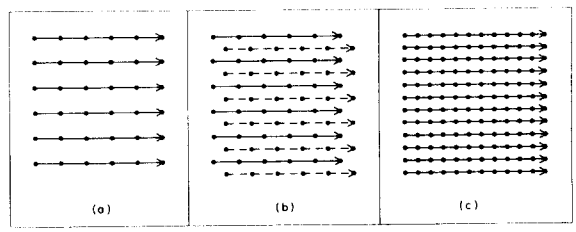

FIG. 1. Schematic diagram illustrating the sampling method used with the three matrix configurations: (a) 512×512 matrix, (b) double-sampling matrix (2×512×512), and (c) 1024×1024 matrix. The dots indicate the sampling locations. For the double-sampling matrix, the second sampling is indicated by the dashed lines.

 0094-2405/88/030384-07$01.20

four times as many are obtained with the 1024×1024 matrix.

We used the digital optical transfer function (OTF) to characterize the resolution properties arising from each of these matrix configurations. The OTF, defined as the two-dimensional Fourier transform of a point spread function (PSF), consists of two components: the MTF and the phase transfer function (PTF) which correspond to the modulus and phase of the complex function, respectively.[11] The digital OTF is defined as the two-dimensional Fourier transform of a digitized (or sampled) PSF. Due to the discrete sampling, which is inherent in all digital imaging systems, the digital OTF depends on the position of the sampling coordinates relative to the position of the PSF.

A. Conventional 512×512 matrix

The two-dimensional digital OTF of a digital radiographic imaging system can be given by

$$\mathrm{OTF}(u,v) = [\mathrm{OTF}_A(u,v)\mathrm{OTF}_S(u,v)] * \left(\exp[-j2\pi(au+bv)] \times \sum_{m,n=-\infty}^{\infty}\sum \delta(u-m/\Delta x, v-n/\Delta y)\right), \quad (1)$$

where $\mathrm{OTF}_A(u,v)$ represents the OTF of the detector system and geometric unsharpness, and $\mathrm{OTF}_S(u,v)$ represents the spatial frequency response of the sampling aperture.[1-3] Their product will be referred to as the presampling OTF and denoted by $\mathrm{OTF}_P(u,v)$. The effect of discrete sampling is expressed in Eq. (1) by the convolution (*) of $\mathrm{OTF}_P(u,v)$ with the Fourier transform of the two-dimensional sampling function, which consists of a two-dimensional array of Dirac delta functions at sampling distance intervals of Δx and Δy in the corresponding orthogonal directions. Here, the PSF is centered at the origin and the sampling positions occur at $(a+m\Delta x, b+n\Delta y)$, where m and n are integers. The formulation given in Eq. (1) allows for arbitrary shifting of the sampling coordinate system by (a,b) relative to the PSF (or image distribution) which gives rise to the phase factor. Equation (1) can be reduced to a two-dimensional summation, namely,

$$\mathrm{OTF}(u,v) = \sum_{m,n=-\infty}^{\infty}\sum \exp\{-j2\pi[(am/\Delta x)+(bn/\Delta y)]\} \times \mathrm{OTF}_P(u-m/\Delta x, v-n/\Delta y). \quad (2)$$

We assumed that a sufficient number of quantization levels are available in the analog-to-digital (A/D) conversion, and thus that the effect of quantization on the digital OTF is negligible.

We examined the digital OTF at two extreme alignments of the sampling coordinates relative to the PSF, namely, a center alignment and a shifted alignment. The center alignment occurs when the center of the PSF coincides with the center of the sampling aperture, i.e., $a=b=0$ in Eq. (2). Equation (2) can then be reduced to[3,6]

$$\mathrm{OTF}_C(u,v) = \sum_{m,n=-\infty}^{\infty}\sum \mathrm{OTF}_P(u-m/\Delta x, v-n/\Delta y) = \sum_{m,n=-\infty}^{\infty}\sum \mathrm{OTF}_P(u-2mu_N, v-2nv_N), \quad (3)$$

where the Nyquist frequency (u_N, v_N)[12,13] is defined as the reciprocal of twice the sampling distance (i.e., $u_N = 1/2\Delta x$ and $v_N = 1/2\Delta y$). Aliases of $\mathrm{OTF}_P(u,v)$ are centered at integer multiples of twice the Nyquist frequency in each orthogonal direction. In Fig. 2(a), these aliases in the spatial frequency domain are represented schematically by circles. It should be noted, however, that the presampling OTF is not necessarily isotropic. If the presampling OTF is not zero at and beyond the Nyquist frequency, overlapping portions will sum together, producing an aliasing effect.[13] The increase in the digital OTF resulting from the summation of overlapped portions of the presampling OTF does not, however, correspond to a true increase in the resolution properties of the system.

The shifted alignment results when the center of the sampling aperture is shifted from the center of the PSF by one-half the sampling distance in each orthogonal direction, i.e., $a=\Delta x/2, b=\Delta y/2$ in Eq. (2). The digital OTF for this shifted alignment case is obtained from Eq. (2), namely,[3,6]

$$\mathrm{OTF}_{SH}(u,v) = \sum_{m,n=-\infty}^{\infty}\sum (-1)^{m+n}\mathrm{OTF}_P(u-2mu_N, v-2nv_N). \quad (4)$$

Aliases of the presampling OTF are shown schematically in Fig. 2 (b), where the positive and negative aliases are represented by solid and dashed circles, respectively.

B. Double-sampling matrix

One method of reducing the aliasing effect is to decrease the sampling distance, and consequently to increase the Nyquist frequency. This is, in effect, accomplished with a double-sampling technique in which the image is sampled a second time at positions shifted by one-half the pixel size from the positions of the first sampling. That is, by double-sampling an image with a 512×512 matrix and then interpolating, one can obtain a synthesized 1024×1024 image.

The digital OTF for the double-sampling matrix can be calculated by averaging of the two digital OTF's for the two alignments of the conventional 512×512 matrix. The center alignment for the double-sampling technique corresponds to 512×512 sampling at positions $(m\Delta x, n\Delta y)$ and also at $(\Delta x/2+m\Delta x, \Delta y/2+n\Delta y)$, i.e., at the center and shifted alignments, respectively, of the conventional 512×512 matrix. Thus, the digital OTF for the double-sampling matrix at the center alignment is given by the average of Eqs. (3) and (4), namely,

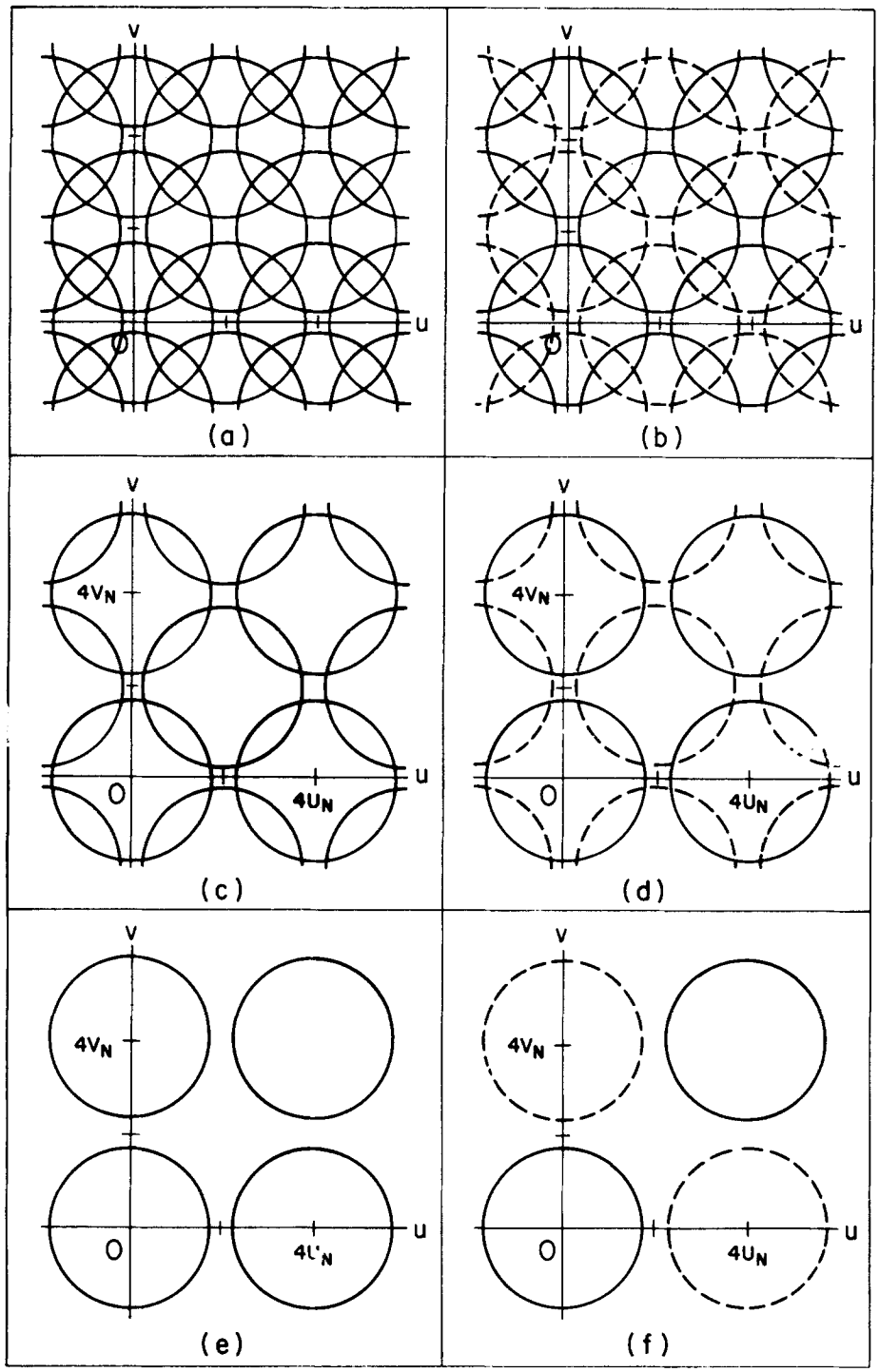

FIG. 2. Schematic diagram illustrating the positions of the aliases of the presampling OTF for the 512×512 matrix [(a) center and (b) shifted alignments], the double-sampling matrix [(c) center and (d) shifted alignments], and the 1024×1024 matrix [(e) center and (f) shifted alignments] in the two-dimensional spatial frequency domain. The positive and negative aliases are represented by the solid and dashed circles, respectively.

$$\mathrm{OTF}_{C,DB}(u,v) = \sum_{m,n=-\infty}^{\infty}\sum \mathrm{OTF}_P(u-4mu_N, v-4nv_N) + \sum_{m,n=-\infty}^{\infty}\sum \mathrm{OTF}_P[u-(4m+2)u_N, v-(4n+2)v_N]. \quad (5)$$

Figure 2(c) illustrates the aliases of the presampling OTF which arise with this center alignment of the double-sampling matrix.

The double-sampling matrix at the shifted alignment corresponds to sampling at $(\Delta x/2 + m\Delta x, n\Delta y)$ and at $(m\Delta x, \Delta y/2 + n\Delta y)$. Substituting into Eq. (2) for each of the sampling locations, i.e., $a = \Delta x/2, b = 0$ and $a = 0, b = \Delta y/2$, and then averaging, we obtain the digital OTF for the double-sampling matrix at the shifted alignment, namely,

$$\mathrm{OTF}_{SH.DB}(u,v) = \sum_{m,n=-\infty}^{\infty}\sum \mathrm{OTF}_P(u-4mu_N, v-4nv_N) - \sum_{m,n=-\infty}^{\infty}\sum \mathrm{OTF}_P[u-(4m+2)u_N, v-(4n+2)v_N]. \quad (6)$$

The aliases which result with this shifted alignment are demonstrated in Fig. 2 (d). For the double-sampling matrix [Figs. 2 (c) and 2(d)], the aliases overlap to a lesser extent than do those for the conventional 512×512 matrix, because of the increased spacing between aliases. In fact, along the orthogonal spatial frequency axes (u and v), the effective Nyquist frequency has been doubled. It should be noted that the OTF's expressed by Eqs. (5) and (6) do not include the contribution of the interpolation which is performed in order to synthesize a 1024×1024 image with the double-sampling technique.

C. High-resolution 1024×1024 matrix

If the sampling matrix size is increased by a factor of 2 in each orthogonal direction, then the sampling distance is decreased by a factor of 2 and consequently the Nyquist frequency is increased by a factor 2. The digital OTF's for the high-resolution matrix (1024×1024), at the center and shifted alignments, can be expressed by Eqs. (3) and (4), respectively, where u_N and v_N are now twice as large. The aliases of the presampling OTF are illustrated in Figs. 2(e) and 2(f) for the center and shifted alignments, respectively. Among the three matrix configurations, the high-resolution matrix causes aliases of the presampling OTF to occur at the greatest intervals in the spatial frequency domain. It is important to note, however, that the presampling OTF for the high-resolution matrix may differ from that used in the conventional 512×512 matrix and double-sampling matrix techniques if a small sampling aperture is employed.

III. METHODS

The resolution properties obtainable with each of the three matrix configurations were compared theoretically, by simulating the corresponding OTF's, and also experimentally, by using radiographic phantoms. The digital radiographic imaging system employed was a Siemens Digitron 2 DSA system. This system included a Garantix 1000 x-ray generator with a 0.6-mm focal spot x-ray tube, a triple-mode (12, 17, and 25 cm) Optilux RBV 25/17 HN CsI (Tl) image intensifier with grid (12:1, 40 lines/cm), and a Videomed N (525-line) TV system. In addition, film images could be obtained with a 100-mm camera attached to the II output. The Digitron 2 unit contained a 10-bit A/D converter, a 20-megabyte semiconductor memory, and an 80-megabyte Winchester disk for storage of image data. For image analysis, data were transferred on magnetic tape to a DEC VAX 11/750 computer system which is interfaced to two Gould FD 5000 (512×512) image processors and two Ramtek 9460 high-resolution (1024×1024) image processors.

The Digitron 2 included logarithmic amplification prior to A/D conversion. A 512×512 matrix and the 12-cm II mode were used in this study. For this set of parameters, the effective pixel size (i.e., the sampling distance in this case) was found to be 0.32 mm. Actually, the effective pixel size was approximately 7% larger in the horizontal direction (i.e., parallel to the TV raster lines) than in the vertical direction. However, we averaged the two values for simplicity.

For the calculations in the simulation studies, the MTF of the II itself and the presampling MTF of the II–TV digital imaging system were needed. The MTF of the II itself was measured from exposures of a 0.05-mm-wide slit placed on the II input plane. Film images of the slit were obtained with the 100-mm camera and Kodak XGR film, and subsequently scanned with a microdensitometer. The Fourier transform of the corresponding line spread function yielded the MTF of the II by a technique used for conventional screen/film combinations.[7,8] For the purpose of linearization, the sensitometric data for the XGR film were measured with a DuPont Cronex sensitometer. Degradation in the MTF caused by the optical system and the film was assumed to be negligible. The measured MTF of the II is shown in Fig. 3. We found no significant difference between the MTF's measured in the horizontal and vertical directions.

The presampling MTF of the digital imaging system was measured for digital images of a 0.05-mm-wide slit that was positioned on the II input plane, at a small angle relative to the TV raster lines.[6] This angulated slit technique allowed us to determine the presampling MTF up to twice the Nyquist frequency of the system. The characteristic curve[14] of the DSA system was employed as a means of linearization. The measured presampling MTF is also shown in Fig. 3. It should be noted that the presampling MTF becomes zero at frequencies prior to twice the Nyquist frequency for the 512×512 matrix.

A. Simulation studies

Digital MTF's were calculated for the three matrices at both the center and shifted alignments. The measured presampling MTF shown in Fig. 3 was used for the OTF_P term in Eqs. (3)–(6) in the calculations for the conventional 512×512 matrix and for the double-sampling matrix. For the high-resolution 1024×1024 matrix, OTF_P was obtained from the product of the MTF of the II–TV system (OTF_A)

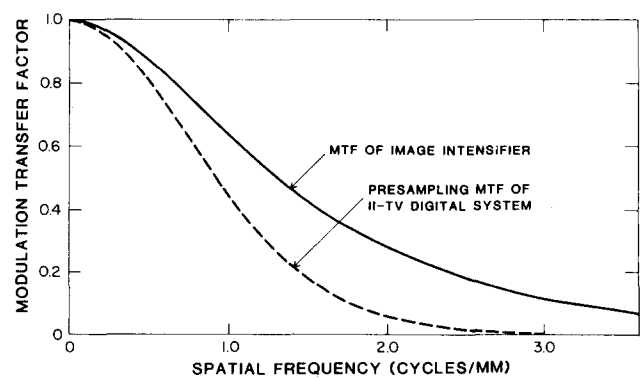

FIG. 3. MTF of the II in the 12-cm mode, and presampling MTF of the II–TV digital system used with 512×512 acquisition.

and the spatial frequency response (OTF_S) of the corresponding 0.16-mm sampling aperture (i.e., one-half the pixel size of the 512×512 matrix). The MTF of the II–TV system (OTF_A) was estimated from the measured presampling MTF (Fig. 3) divided by the spatial frequency response OTF_S of the 0.32-mm sampling aperture. We have assumed a square pixel in which the sampling distance equals the size of the uniform square sampling aperture. Thus, the spatial frequency response of the square aperture is the corresponding sinc function in the frequency domain. In order to simulate the aliasing effect on the OTF accurately, we included 120 aliases (11 by 11 array) plus the presampling OTF in the summation.

In a second simulation study, we employed a hypothetical radiographic imaging system with improved resolution by assuming that the MTF of the TV camera is unity. Thus, the presampling OTF corresponded to the product of the MTF of the II (Fig. 3) and the spatial frequency response of the corresponding sampling aperture for the three matrices investigated.

B. Phantom image studies

In order to make a qualitative comparison of the effect of the three matrix configurations on image resolution, we obtained images of a star pattern phantom and a hand phantom by using the Digitron 2 system. Double sampling was achieved with a precision device which we used to shift the phantom in a direction diagonal to that of the TV raster lines. The precision and accuracy of this moving device are approximately 10 μ. The 1024×1024 image resulting from the use of a double-sampling matrix was synthesized from two 512×512 image frames—one with the phantom at an arbitrary starting position and another with the phantom in a position at a distance of $\Delta x/\sqrt{2}$ along the diagonal direction; that is, the 512×512 sampling coordinates remained stationary, and the phantom was shifted by $(\Delta x/2, \Delta y/2)$, where we assumed $\Delta x = \Delta y$. The resulting 1024×1024 image was synthesized in the spatial domain by linear interpolation of the four adjacent pixel values, which yielded the remaining data points. We compared this 1024×1024 image obtained from the double-sampling technique with the image made with the conventional 512×512 matrix by enlarging the 512×512 image (i.e., either of the original image frames) by a factor of 2 in each orthogonal direction.

Simulated images for the high-resolution 1024×1024 matrix were obtained with the 100-mm camera connected to the output of the II. We used a Fuji drum scanner[15] to digitize the film image with a pixel size of 0.1 mm. This pixel size on the film plane of the 100-mm camera approximately equals the effective pixel size obtained with a 1024×1024 matrix.

IV. RESULTS

Digital MTF's of the three matrix configurations at the center and shifted alignments are shown in Figs. 4(a) and 4(b) along the horizontal and diagonal spatial frequency axes, respectively. Although the digital MTF's were obtained from two-dimensional calculations, they are shown here in one dimension for simplicity of illustration.

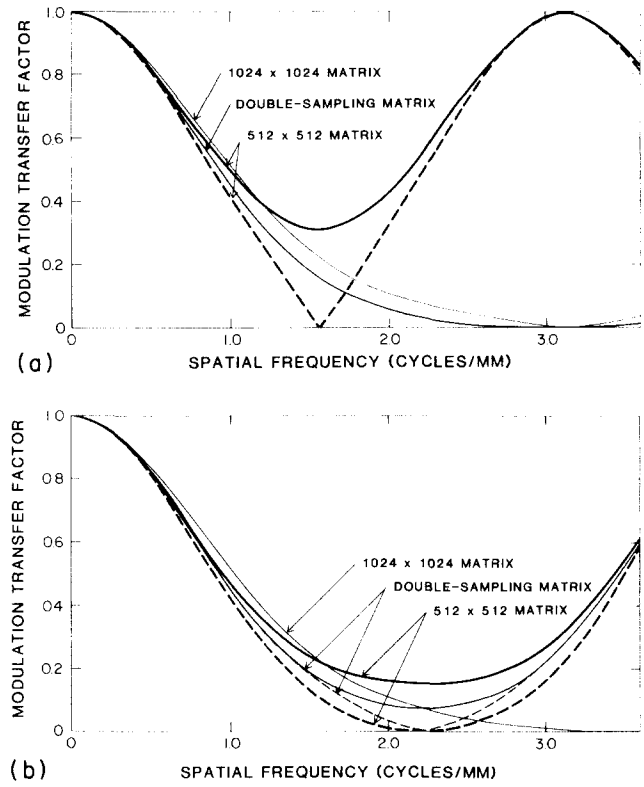

FIG. 4. Calculated digital MTF's of the II–TV digital imaging system along the (a) horizontal and (b) diagonal spatial frequency axes for the three matrix configurations. Solid and dashed curves correspond to the center and shifted alignments, respectively.

As expected, the largest aliasing effect occurs with the 512×512 matrix, and subsequently the variation between the digital MTF's for the center and shifted alignments is greatest (because digital imaging systems are not shift invariant). For the double-sampling matrix, the Nyquist frequency along the horizontal axis extends to twice that for the 512×512 matrix, and thus the aliasing effect is reduced substantially, since the presampling OTF approaches zero prior to twice the Nyquist frequency of the 512×512 matrix (see Fig. 3). Along the diagonal direction, the Nyquist frequency is the same for the 512×512 and double-sampling matrices. However, a larger aliasing effect occurs with the 512×512 matrix because of the presence of additional aliases along the horizontal and vertical axes, which contribute to the summation (see Fig. 2). The 1024×1024 matrix provides a higher MTF because of the small sampling distance (which increases the Nyquist frequency) and because of the sampling aperture, which is smaller by a factor of 2 than that used for the other two matrix configurations (i.e., less blurring prior to sampling). However, this improvement in the resolution is *relatively small* which suggests that the II, lens system, and/or TV camera in the imaging chain may limit the resolution properties of this system.

Figures 5(a) and 5(b) illustrate the digital MTF's along the horizontal and diagonal directions, respectively, for the hypothetical "improved" digital imaging system in which the resolution degradations caused by the lens system and TV camera are assumed to be negligible. The two-dimensional calculations for the center and shifted alignments

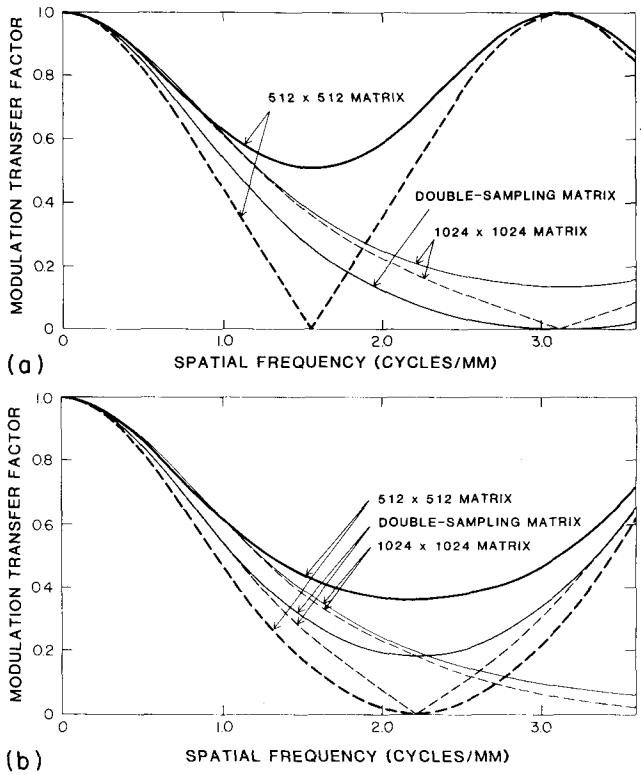

FIG. 5. Calculated digital MTF's of the "improved" system along the (a) horizontal and (b) diagonal spatial frequency axes for the three matrix configurations. Solid and dashed curves correspond to the center and shifted alignments, respectively.

were performed with the measured MTF of the II used for OTF_A, as described earlier. Because of the high level of the presampling MTF with this "improved" system, a large aliasing effect occurs as compared to that of the actual system. It should be noted that the pixel sizes of the two systems (illustrated in Figs. 4 and 5) are the same; only the presampling MTF's differ. It is apparent from a comparison of Figs. 4 and 5 that the reduction in the aliasing effect by use of the double-sampling matrix, instead of the 512×512 matrix, is greater with the improved system than with the present system. Furthermore, the expected increase in the digital MTF caused by the use of the 1024×1024 matrix also is greater with this improved system.

Star pattern images for the 512×512 matrix, double-sampling matrix, and 1024×1024 matrix are shown in Figs. 6(a), 6(b), and 6(c), respectively. The aliasing effect is readily seen in the star pattern image in Fig. 6(a). The increased resolution achieved with the double-sampling technique is apparent in the comparison of the star pattern images of Figs. 6(a) and 6(b). Also, this improvement in resolution with the double-sampling matrix as compared to the 512×512 matrix appears to be larger in the horizontal and vertical directions than in the diagonal direction, as predicted from the simulation studies. The resolution in the star pattern image obtained with the 1024×1024 configuration [Fig. 6 (c)] is improved significantly over that in the images in Figs. 6(a) and 6(b). However, the image is very noisy; this is attributable to the film graininess in the image obtained with the 100-mm camera.

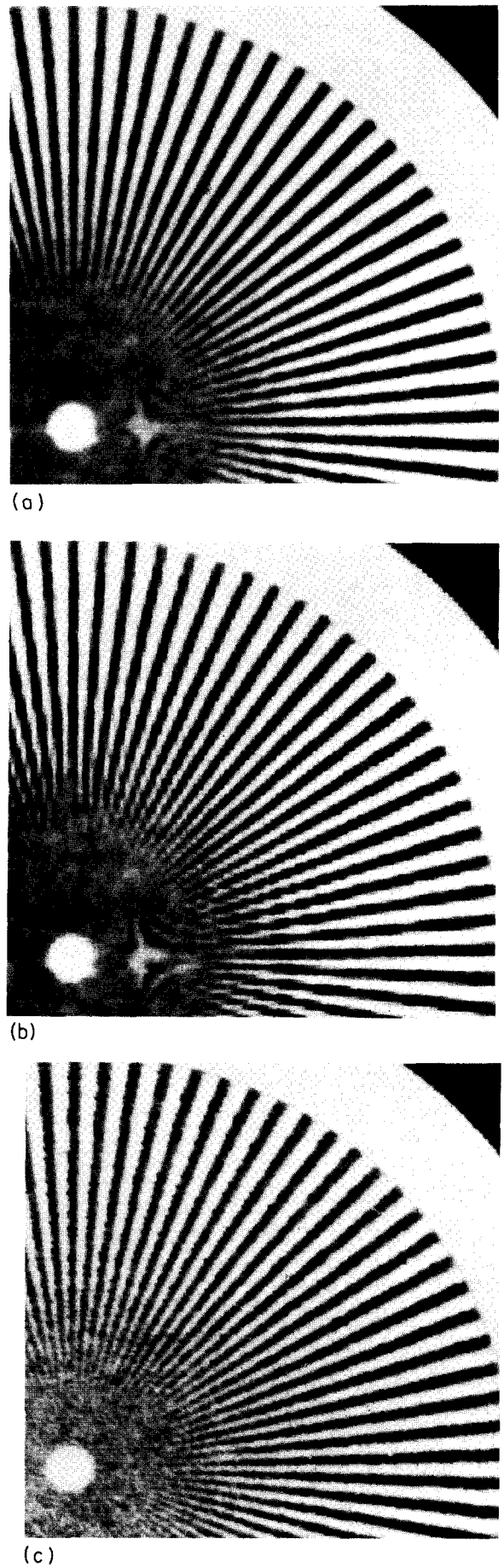

FIG. 6. Star pattern images obtained with (a) the 512×512 matrix, (b) the double-sampling matrix, and (c) the high-resolution 1024×1024 matrix.

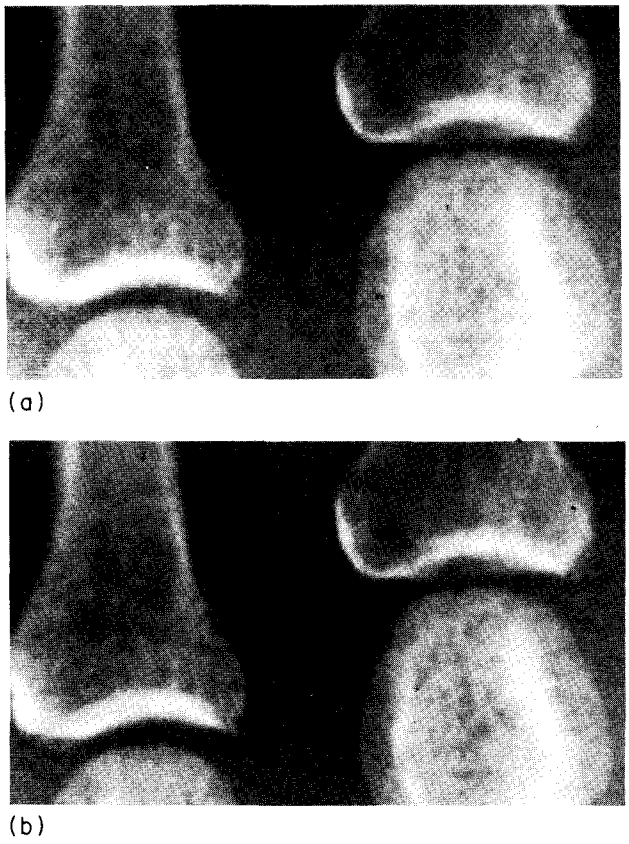

FIG. 7. Hand phantom images obtained with (a) the 512×512 matrix and (b) the double-sampling matrix.

Images of the hand phantom are shown in Figs. 7(a) and 7(b) for the 512×512 matrix and the double-sampling matrix, respectively. The improvement in resolution with the double-sampling technique is much more subtle in the comparison of these hand phantom images than in that of the star pattern images. A slight improvement, however, is noticeable at the edges of the bones in Fig. 7(b).

V. DISCUSSION AND CONCLUSION

We have investigated the effects of three matrix configurations (512×512, double-sampling, 1024×1024) on the resolution of an II–TV digital imaging system. In calculating the two-dimensional digital MTF for each matrix configuration, we used the measured MTF's of the analog components (II, TV) and the specific digital parameters of the imaging system. It should be noted that, because a digital imaging system is not shift invariant, the digital MTF needs to be interpreted cautiously in conjunction with the corresponding presampling MTF. Results of both the simulation studies and the comparison of phantom images with our present II–TV digital system showed only small improvements in the resolution as the matrix configuration was changed from 512×512 to double sampling and then to 1024×1024. However, substantial differences in resolution resulted in the simulation study when the MTF of the TV system was assumed to be unity. This indicates that the factors limiting the resolution in our present II–TV digital system are the analog components prior to sampling. Thus, the significant advantage of upgrading an existing II–TV digital imaging system to 1024×1024 matrix acquisition can be realized only when the resolution capabilities of the TV camera system are improved.

In our investigation, we studied a double-sampling matrix configuration. It is important to note that the increase in resolution that is achieved by conversion from a conventional 512×512 matrix to a double-sampling matrix is not the same in all directions. The greatest improvement in resolution is obtained in the directions perpendicular and parallel to the TV raster lines. In addition, the double-sampling approach can be implemented either by shifting of the sampling coordinate system or by shifting of the object being imaged. For example, the sampling coordinate system could be shifted by switching electronically the scanning pattern of the TV camera or by moving mechanically the II–TV system. For a stationary sampling coordinate system, the object holder or the patient table could be shifted mechanically between two exposures. This double-sampling approach has the potential of yielding higher-resolution images with systems which have high-resolution analog components, but are limited to 512×512 matrix acquisition.

ACKNOWLEDGMENTS

The authors are grateful to Y. Kume who provided the MTF data for the II (Fig. 3), C. E. Metz and G. Powell for their discussions, C. A. Blanck for her technical assistance, E. Lanzl for editing the manuscript, and E. Ruzich for her secretarial assistance. This work was supported by USPHS Grant No. CA 24806.

[a] Present address: Department of Electrical Engineering, Gifu Technical College, Motosu-gun, Gifu 501-04, Japan.

[1] M. L. Giger and K. Doi, Med. Phys. **11**, 287 (1984).
[2] M. L. Giger and K. Doi, in *Recent Developments in Digital Imaging*, edited by K. Doi, L. Lanzl, and P.-J. Lin (American Institute of Physics, New York, 1985).
[3] M. L. Giger, Ph.D. dissertation, University of Chicago, 1985.
[4] A. S. Gomes, P. J. Papin, N. J. Mankovich, and J. F. Lois, Am. J. Roentgenol **146**, 835 (1986).
[5] M. Kamiya, F. Takahashi, M. Tsuneoka, T. Hayashi, H. Yokouchi, and M. Takahashi, SPIE **626**, 366 (1986).
[6] H. Fujita, K. Doi, and M. L. Giger, Med. Phys. **12**, 713 (1985).
[7] K. Doi, G. Holje, L.-N. Loo, H.-P. Chan, J. M. Sandrik, R. J. Jennings, and R. F. Wagner, "MTF's and Wiener Spectra of Radiographic Screen–Film Systems," HHS Pub. (FDA) 82-8187, 1982.
[8] K. Doi, Y. Kodera, L.-N. Loo, H.-P. Chan, Y. Higashida, and R. J. Jennings, "MTF's and Wiener Spectra of Radiographic Screen–Film Systems," Vol. II, HHS Publication (FDA) 86-8257, 1986.
[9] R. A. Sones and G. T. Barnes, Med. Phys. **11**, 166 (1984).
[10] R. T. Droege and M. Rzeszotarski, Med. Phys. **12**, 721 (1985).
[11] C. E. Metz and K. Doi, Phys. Med. Biol. **24**, 1079 (1979).
[12] E. O. Brigham, *The Fast Fourier Transform* (Prentice–Hall, Englewood Cliffs, NJ, 1974).
[13] R. N. Bracewell, *The Fourier Transform and its Aplications*, (McGraw–Hill, New York, 1978).
[14] H. Fujita, K. Doi, M. L. Giger, and H.-P. Chan, Med. Phys. **13**, 13 (1986).
[15] M. Ishida, H. Kato, K. Doi, and P. H. Frank, SPIE **347**, 42 (1982).